THE JOURNAL OF PHYSICAL CHEMISTRY A
A JOURNAL OF THE AMERICAN CHEMICAL SOCIETY

pubs.acs.org/JPCA
Article

Biogenic and Anthropogenic Secondary Organic Aerosols Become Fluorescent after Highly Acidic Aging

Published as part of The Journal of Physical Chemistry A special issue "Vicki H. Grassian Festschrift".

Cynthia Wong, Jett Vuong, and Sergey A. Nizkorodov*

Cite This: J. Phys. Chem. A 2024, 128, 7657−7668
Read Online
ACCESS | Metrics & More | Article Recommendations

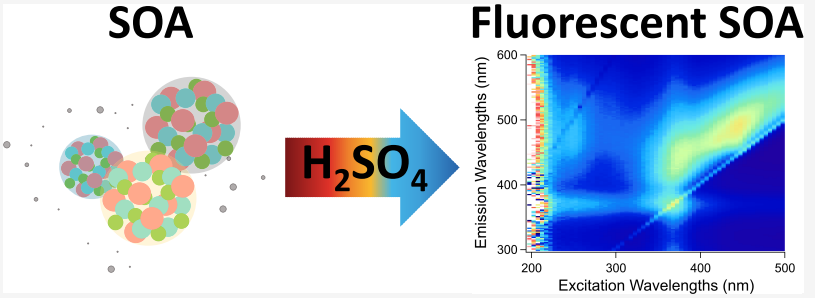

ABSTRACT: Primary biological aerosol particles (PBAPs) and secondary organic aerosol (SOA) both contain organic compounds that share similar chemical and optical properties. Fluorescence is often used to characterize PBAPs; however, this may be hindered due to interferences from fluorophores in SOA. Despite extensive efforts to understand the aging of SOA under elevated particle acidity conditions, little is known about how these processes affect the fluorescence of SOA and thereby their interference with the measurements of PBAPs. The objective of this study is to investigate the fluorescence of SOA and understand the influence of acidity on the optical properties of organic aerosols and potential interference for the analysis of bioaerosols. The SOA was generated by O_3- or OH-initiated oxidation of d-limonene or α-pinene, as well as by OH-initiated oxidation of toluene or xylene. The SOA compounds were then aged by exposure to varying concentrations of aqueous H_2SO_4 for 2 days. Absorption and fluorescence spectrophotometry were used to examine the changes in the optical properties before and after aging. The key observation was the appearance of strongly light-absorbing and fluorescent compounds at pH = ∼−1, suggesting that acidity is a major driver of SOA aging. The aged SOA from biogenic precursors (d-limonene and α-pinene) resulted in stronger fluorescence than the aged SOA from toluene and xylene. The absorption spectra of the aged SOA changed drastically in shape upon dilution, whereas the shapes of the fluorescence spectra remained the same, suggesting that the fluorophores and chromophores in SOA are separate sets of species. The fluorescence spectra of aged SOA overlapped with the fluorescence spectra of PBAPs, suggesting that SOA exposed to highly acidic conditions can be confused with PBAPs detected by fluorescence-based methods. These processes are likely to play a role in the atmospheric regions where high concentrations of H_2SO_4 persist, such as the upper troposphere and lower stratosphere.

INTRODUCTION

Our understanding of the extent to which aerosols contribute to global climate change is still limited. Organic aerosols, which include bioaerosols (also known as primary biological aerosol particles, PBAPs) and secondary organic aerosol (SOA), account for a dominant fraction of particulate matter in the lower troposphere and can heavily influence the air quality and radiative forcing.[1] PBAPs contain biological components such as bacteria, viruses, fungi, and biological molecules,[2] while secondary organic aerosols are formed from the oxidation of biogenic and anthropogenic volatile organic compounds (VOCs).[3,4]

PBAPs and SOA are extremely complex, and both contain organic compounds that share similar chemical and optical properties, including the ability to fluoresce.[5] Many atmospheric organic species with significant conjugation of π-bonds, including amino acids with aromatic functional groups (e.g., tryptophan), vitamins, and humic-like substances, have been identified as efficient fluorophores.[6−8] The ability to detect and analyze these fluorophores using fluorescence spectroscopy has proved useful for understanding the chemical composition,

Received: June 27, 2024
Revised: August 16, 2024
Accepted: August 20, 2024
Published: August 30, 2024

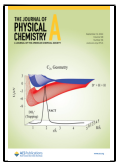

https://doi.org/10.1021/acs.jpca.4c04287
J. Phys. Chem. A 2024, 128, 7657−7668

Table 1. Aging Experiment Summary

SOA precursor	oxidant	collection time (h)	mass of SOA extracted in segment (mg)	estimated concentration of H_2SO_4	effective pH = −log[H^+]
APIN	O_3	3.5	0.951		
APIN	O_3	3.5	0.974	0.52 mM	3.0
APIN	O_3	3.5	1.110	10 M	−1.1
LIM	O_3	3.3	1.036		
LIM	O_3	3.3	1.243	0.52 mM	3.0
LIM	O_3	3.3	1.031	10 M	−1.1
APIN	OH	7.2	0.814		
APIN	OH	7.2	0.841	0.52 mM	3.0
APIN	OH	7.2	0.736	10 M	−1.1
LIM	OH	7.3	0.755		
LIM	OH	7.3	0.744	0.52 mM	3.0
LIM	OH	7.3	0.694	10 M	−1.1
TOL	OH	14	0.906		
TOL	OH	14	0.988	0.52 mM	3.0
TOL	OH	14	0.887	10 M	−1.1
XYL	OH	14	0.583		
XYL	OH	14	0.610	0.52 mM	3.0
XYL	OH	14	0.594	10 M	−1.1

sources, and chemical reactions of atmospheric aerosols.[9,10] However, the presence of weakly fluorescent compounds in SOA complicates the applications of fluorescence spectroscopy to quantitative and qualitative analysis of PBAPs, as the interferences of nonbiological particles, such as SOA, can skew the data and conclusions.[7,11−15] This problem is further complicated, as organic aerosols undergo chemical and physical transformations during transport as they are exposed to different environmental conditions, such as acidity.

Acidity of atmospheric particles controls the rates and mechanisms of several multiphase processes, such as acid-catalyzed SOA formation, oxidation of SO_2, and chemical speciation of dissolved species.[16,17] Acidity of the atmospheric aqueous phase can vary significantly. Cloud and fog droplets tend to be less acidic with a pH of +2 to +7, while aerosol particles are more acidic with effective pH values from −1 to +8.[18] This property is dependent on the source of the particles, their chemical composition, and ambient relative humidity (as aerosol liquid water serves to dilute the acids in particles). Particle size is also important—Angle et al. showed that submicron sea-spray particles are more acidic than course-mode particles.[19] Acidity plays a crucial role in many chemical reactions of organic compounds, including those found in SOA. These acid-catalyzed reactions include hemiacetal and acetal formation, hydration of aldehydes and ketones, aldol condensation of carbonyls, esterification of carboxylic acids, and ring opening of epoxides, to name a few.[20] Thus, understanding the role of acidity in the chemical and physical transformation of these complex organic aerosols can provide valuable insights into how acidity impacts their properties, including fluorescence.

Many field studies have reported highly acidic aerosols (with negative pH values), specifically in Southeastern Asia, the Eastern United States, China, and other locations, likely due to the high emissions of SO_2.[21−24] Additionally, stratospheric aerosols have been known to be very acidic, resulting in stratospheric particles that can contain 40−80 wt % H_2SO_4 originating from the injection of SO_2 from volcanic eruptions, resulting in a pH between −0.8 and −1.[25−30] Although there are field observations of acidity levels that are this high, laboratory studies of how SOA ages under these conditions are still limited. A recent study of the α-pinene ozonolysis SOA reported that acidity is a major driver of SOA aging, resulting in a large change in the chemical composition and optical properties of SOA in the presence of concentrated H_2SO_4, including the formation of unidentified fluorophores.[31] This prompts the question of whether other types of biogenic and anthropogenic SOA can become fluorescent after being exposed to highly acidic conditions.

Despite significant efforts to understand the aging of SOA under high-acidity conditions, little is known about how these processes affect fluorescence and thereby their interference with the measurements of PBAPs. Additionally, studying the fluorescence properties of SOA could provide valuable insights into the acid-catalyzed reactions and chemical composition of the fluorophores. The objective of this study is to investigate the excitation−emission spectroscopy of SOA generated from various precursors to understand the influence of the acidity on the optical properties of organic aerosols. We demonstrate that highly acidic conditions due to sulfuric acid, the most abundant acid in the atmosphere, promote acid-catalyzed reactions and thereby form fluorophores in SOA that can interfere with the detection of PBAPs by fluorescent methods.

EXPERIMENTAL METHODS AND MATERIALS

Formation of SOA. Six different types of SOA were studied in this work: α-pinene (Arcos, 98%) ozonolysis (APIN/O_3), d-limonene (Sigma-Aldrich, 99%) ozonolysis (LIM/O_3), α-pinene low-NOx photooxidation (APIN/OH), d-limonene low-NOx photooxidation (LIM/OH), toluene (Fisher, 99%) low-NOx photooxidation (TOL/OH), and *p*-xylene (Sigma-Aldrich, 99%) low-NOx photooxidation (XYL/OH). A summary of all samples made in this study can be found in Table 1. Two types of techniques were used to generate SOA as previously described.[31−33]

In brief, O_3-initated SOA was prepared from the oxidation of D-limonene (LIM) and α-pinene (APIN) by ozone (O_3) using a 20 L continuous-flow reactor. Ozone was generated using a commercial ozone generator (OzoneTech OZ2SS-SS) and introduced into the reactor in a 0.5 slm (standard liters per minute) flow of oxygen. The liquid VOC precursor was injected at 25 μL/h into a 5 slm flow of air. The starting

https://doi.org/10.1021/acs.jpca.4c04287
J. Phys. Chem. A 2024, 128, 7657−7668

concentrations of VOC and O_3 were ∼14 and ∼10 ppm, respectively. A charcoal denuder was used to scrub excess aqueous O_3 from the flow before SOA collection. SOA was collected for about 2 h to achieve a mass of ∼2−4 mg, enough for the analysis described below.

For photooxidation-initiated SOA, a different flow reactor was used as described in previous studies.[33,34] This oxidation flow reactor consisted of an 8 L quartz reaction vessel surrounded by two 254 nm UV lamps inside a Rayonet RPR100 photochemical reactor. To initiate the reaction, pure VOC was injected into dry air flowing at 0.3 slm through the vessel using a syringe pump, where it mixed with 0.7 slm of humidified air and 0.3 slm of flow containing O_3. The UV lamps in the reactor photolyzed O_3, thereby producing OH by reacting $O(^1D)$ with H_2O. The OH radicals subsequently reacted with VOC precursors, and the resulting SOA was collected from the exit tube for up to 14 h to obtain about ∼2−3 mg in mass.

In both cases, the SOA was collected onto stage 7 (0.32−0.56 μm) of a micro-orifice uniform deposit impactor (MOUDI; MSP Corp. model 110-R) for 2−14 h on a foil substrate at a flow of 30 slm. Since the flow from the reactor was lower, the makeup air came from HEPA-filtered laboratory air.

Aging in Sulfuric Acid. The protocol used to age SOA in various acidic conditions followed the previously described procedure.[31] Each SOA substrate was cut into three approximately equal segments, and each segment was then extracted in 4 mL of acetonitrile using a shaker. The acetonitrile was removed with a rotary evaporator at ∼25 °C (no heating was used to prevent evaporation of SOA compounds). Water or a solution containing sulfuric acid was added to the vial to dissolve the SOA residue, resulting in a mass concentration of ∼200 μg/mL. This concentration was chosen to generate sufficient signal to noise for the analysis described below. The SOA extracts were then left to age for 2 days in the dark prior to analysis.

Additional experiments were conducted with SOA aged in 10 M H_2SO_4 (pH −1.1) and then diluted with an acid-free solvent to examine the changes in the fluorescence molecules due to acid−base equilibria. These samples were similarly aged in acid for 2 days before the dilution experiments. Further information on these samples can also be found in Table 2.

Table 2. Solution Acidity in the Dilution Experiments[a]

sample	dilution factor	estimated pH (E-AIM)
control (undiluted)	1	−1.1
1:2 Dilution	2	−0.82
1:3 Dilution	3	−0.65
1:4 Dilution	4	−0.52

[a]SOA samples aged at 10 M H_2SO_4 were diluted in water. pH was estimated using extended aerosol inorganics model (E-AIM) (http://www.aim.env.uea.ac.uk/aim/aim.php).

Spectroscopic Measurements. The aged solutions of SOA were analyzed by using a Cary Eclipse fluorescence spectrometer (Agilent). The parameters used for these experiments mimic past studies of SOA fluorescence in our group.[12,13,31,35,36] The background for the fluorescence spectrum was deionized water, and the samples analyzed were the SOA aged in H_2SO_4 after 2 days (we verified that sulfuric acid solutions without SOA did not fluoresce). The excitation wavelength varied over the 200−500 nm range in 5 nm steps, and the emitted fluorescence was recorded over the 300−600 nm range in 2 nm steps for the excitation−emission spectra at a scan rate of 1200 nm/min, resulting in excitation−emission matrices (EEMs). The fluorescence intensities were corrected for Rayleigh and Raman scattering and inner filter effects using previously described methods and then converted into quinine sulfate units (QSUs).[12,35,36] In brief, the absorption spectrum of the sample of interest was taken into account, and the inner filter effect was corrected by using the following equation, where F_{corr} is the corrected fluorescence intensity, F_{obs} is the observed fluorescence intensity, A_{ex} and A_{em} are the raw absorbance values of the excitation/emission wavelength pair at which the intensity was measured, respectively, and the factor of 0.5 assumes that most of the fluorescence is collected from the middle of a 1.0 cm cuvette.

$$F_{corr} = F_{obs} \times 10^{0.5(A_{ex}+A_{em})} \quad (1)$$

Rayleigh and Raman scattering was addressed by subtracting the appropriate blank EEM from the sample EEM (despite this correction, the EEM plots still contain residual contributions from the first- and second-order Rayleigh scattering). Finally, intensities of the SOA samples were converted to QSUs by dividing the intensities by the corrected fluorescence intensity of QS at the excitation/emission peak of 350/450 nm, in which 1 QSU = 0.1 ppm quinine sulfate in 0.05 M H_2SO_4 solution.

Absorption spectra of the SOA samples were taken with a spectrophotometer (Shimadzu UV-2450). Raw absorbance values were converted to mass absorption coefficient (MAC) values in $cm^2\ g^{-1}$ using the following equation, where A_{10} is the measured base-10 absorbance, C_{mass} (g cm^{-3}) is the concentration of the SOA in solution, and b (cm) is the path length (standard quartz 10 mm cuvettes were used in these experiments):

$$MAC = \frac{A_{10}(\lambda) \times \ln(10)}{b \times C_{mass}} \quad (2)$$

The mass concentration only included the starting mass of SOA in solution; it did not include the masses of any of the products that may have formed during aging.

RESULTS AND DISCUSSION

Fluorescence at Varying Acidities. Excitation−emission spectra of organic compounds in environmental samples are often presented as a three-dimensional (3D) EEM, which displays the intensity on a contour plot as a function of the excitation and emission wavelengths.[36,37] Figure 1 shows the EEM plots for APIN/O_3 and LIM/O_3 SOA aged in H_2O, 0.52 H_2SO_4 (pH 3.0), and 10 M H_2SO_4 (pH −1.1) for 2 days. In the control studies for APIN/O_3 (Figure 1a) and LIM/O_3 (Figure 1d), there is no evidence of fluorescence in the SOA mixture, as the intensities are low throughout the entire excitation wavelength range. This finding is consistent with previous work by Bones et al. and Lee et al., who reported no fluorescence in their respective controls for LIM/O_3 and APIN/O_3, and further supported by previous study by Wong et al., who showed that water does not have a significant influence on the chemical aging in SOA.[11,13,32] Aging of SOA in 0.52 H_2SO_4 (pH 3.0) results in plots (Figure 1b,e) that look very similar to the nonacidified controls, with no evidence of fluorophores appearing in the SOA. This indicates that moderately acidic conditions do not promote chemical

https://doi.org/10.1021/acs.jpca.4c04287
J. Phys. Chem. A 2024, 128, 7657−7668

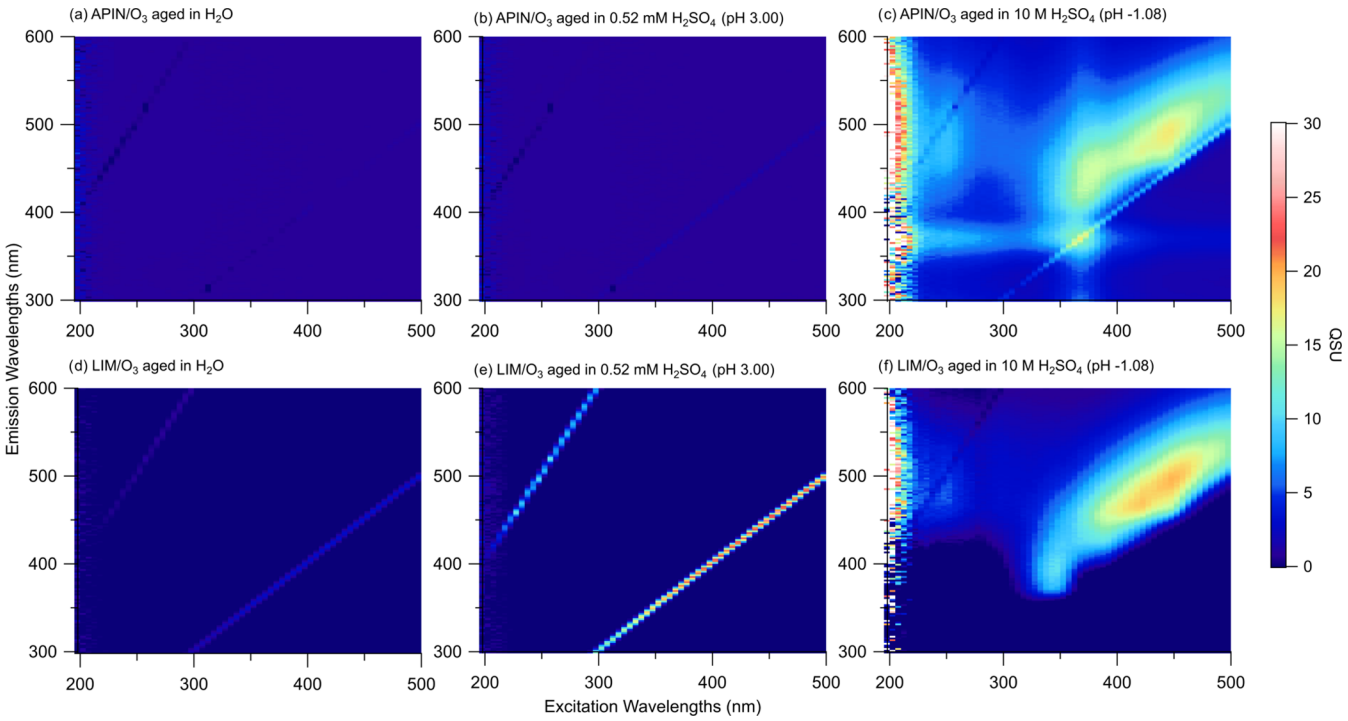

Figure 1. Excitation−emission matrix (EEM) plots for APIN/O_3 and LIM/O_3 SOA aged in H_2O, 0.52 H_2SO_4 (pH 3.0), and 10 M H_2SO_4 (pH −1.1) for 2 days. The color bars in this and remaining EEM plots correspond to quinine sulfate units (QSUs).

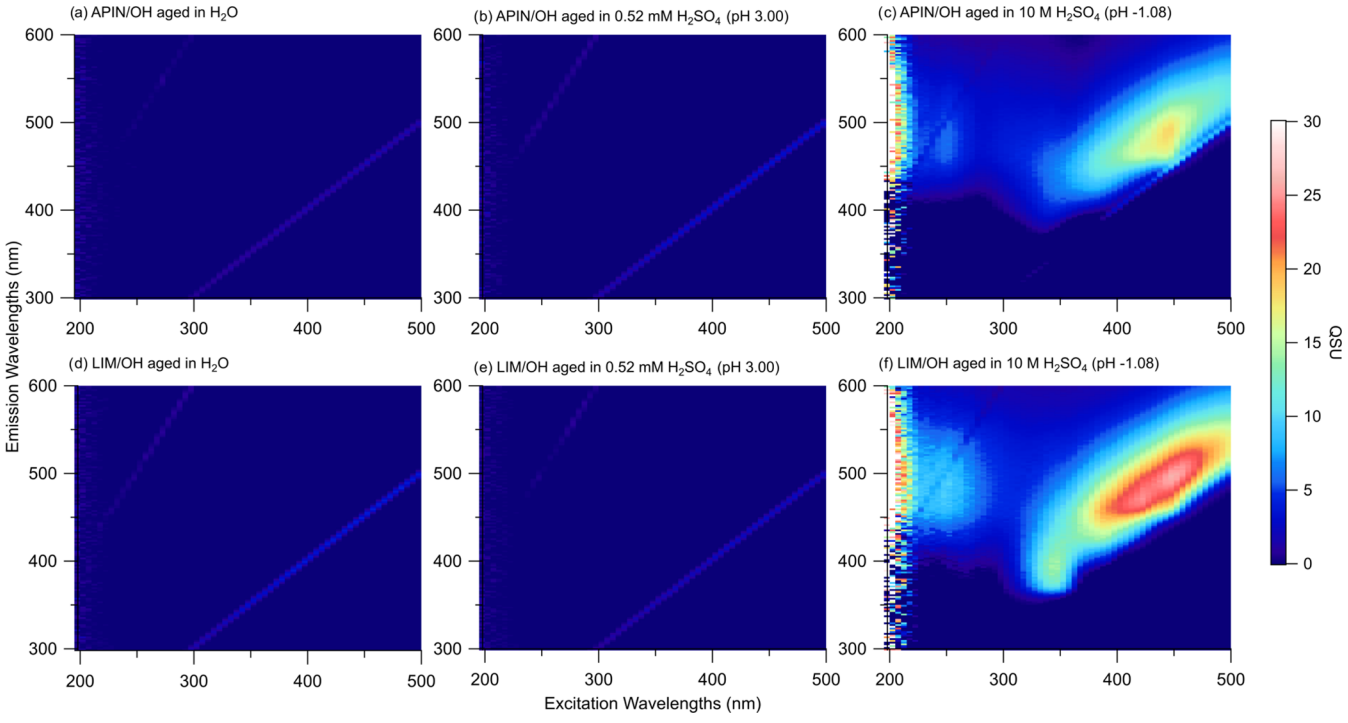

Figure 2. EEM plots for APIN/OH and LIM/OH SOA aged in H_2O, 0.52 M H_2SO_4 (pH 3.0), and 10 M H_2SO_4 (pH −1.1) for 2 days.

reactions that lead to fluorescent compounds, which is consistent with no change in the chemical composition of SOA at pH 3 reported in a previous study.[31] However, when the SOA is aged in 10 M H_2SO_4 (pH −1.1), the plots look notably different (Figure 1c,f). For APIN SOA, there are four main regions: a strong peak with E_x/E_m at 350−500/450−575 nm, a moderately strong peak at E_x/E_m = 350−375/350−400 nm, and two weaker peaks at E_x/E_m = < 275/450−550 nm and E_x/E_m = < 300/350−400 nm. For LIM/O_3, there are only three regions that exhibit fluorescence: a strong peak at E_x/E_m = 350−500/400−575 nm, a moderately strong peak (tail) at E_x/E_m = 330−360/375−425 nm, and finally a weak peak at E_x/E_m = 200−275/425−550 nm. The appearance of these peaks indicates that aging these SOA samples in acid promotes reactions, leading to the formation of fluorophores.

https://doi.org/10.1021/acs.jpca.4c04287
J. Phys. Chem. A 2024, 128, 7657−7668

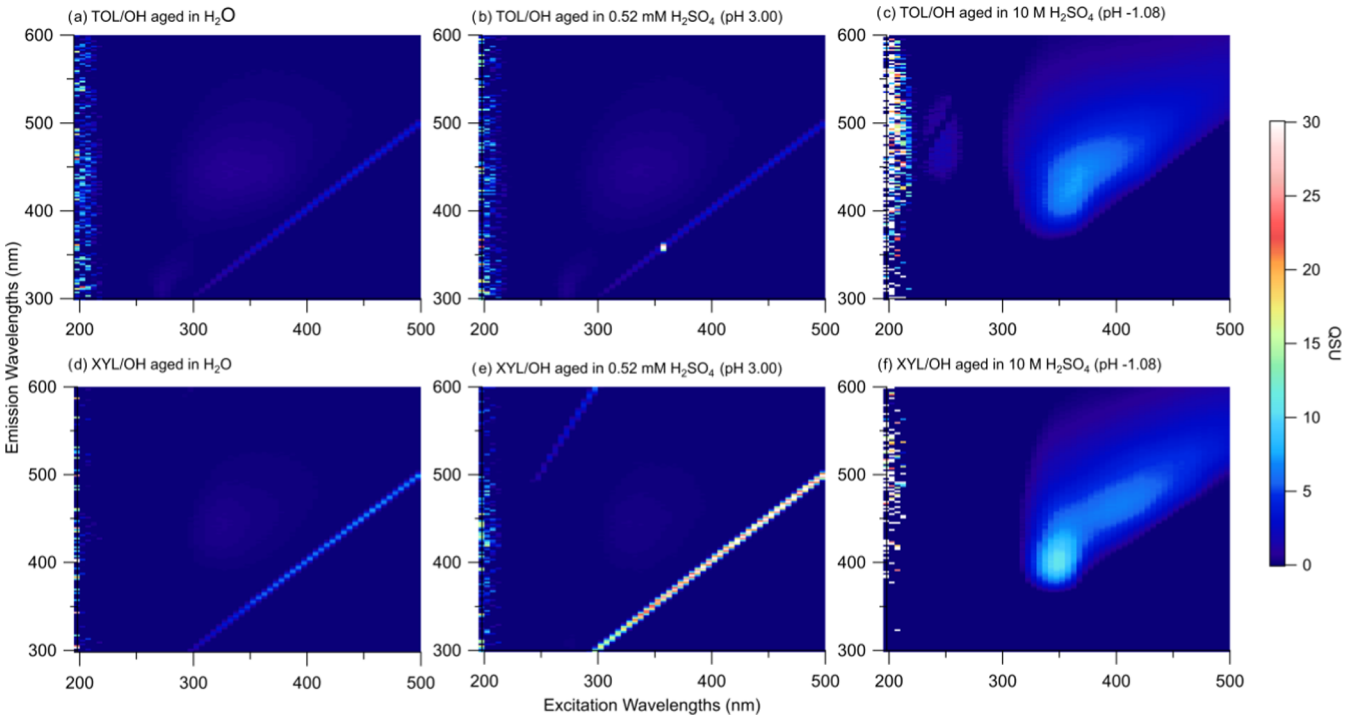

Figure 3. EEM plots for TOL/OH and XYL/OH SOA aged in H_2O, 0.52 M H_2SO_4 (pH 3.0), and 10 M H_2SO_4 (pH −1.1) for 2 days.

The same experiments were repeated for APIN/OH and LIM/OH to examine the role of the oxidant in the formation of fluorophores from biogenic precursors. Similar to the case with the ozonolysis SOA, the unacidified control (Figure 2a,d) and samples aged in moderately acidic conditions (pH 3) do not produce any fluorophores, whereas the highly acidic conditions result in fluorescent solutions. For APIN/OH samples, there are two regions where the sample fluorescence is observed: a strong peak at E_x/E_m = 350−500/450−575 nm and a weak peak at E_x/E_m = 250/450−500 nm. On the other hand, LIM/OH has three regions in the EEM: a strong peak at E_x/E_m = 350−500/400−575 nm, a moderate peak (tail) at E_x/E_m = 325−360/350−400 nm, and a weaker peak at E_x/E_m = 200−300/450−550 nm.

In all systems, fluorophores do not form until the SOA samples are exposed to highly acidic conditions. However, the resulting fluorescence spectra are different for the APIN and LIM SOA, except for the shared strong peak at E_x/E_m = 350−500/400−575 nm. Although both APIN and LIM are monoterpenes ($C_{10}H_{16}$), they have different structures, resulting in oxidation products of APIN being more sterically constrained. This subtle difference in molecular rigidity accounted for the vastly different reactivity of APIN and LIM SOA with ammonia and amines,[38] and this difference in molecular rigidity may also be responsible for the difference in fluorescent properties of acid-aged SOA.

In the LIM/OH and LIM/O_3 systems, both samples showed the same fluorescence peaks but at different intensities. The LIM/OH SOA (Figure 2f) has a fluorescence intensity higher than that of the LIM/O_3 SOA (Figure 1f), despite both samples having the same mass concentration, suggesting that the concentration of fluorophores in the LIM/OH SOA was higher than that in the LIM/O_3 SOA. Additionally, the relative intensities of the fluorescence regions within the EEM could give us insights into the composition of these fluorophores. The peaks at E_x/E_m = 350−500/400−575 nm and E_x/E_m = 200−300/450−550 nm are indicative of highly oxygenated compounds, while the peak at E_x/E_m = 325−360/350−400 nm corresponds to less oxygenated molecules.[39] Based on this classification, it seems that both LIM/OH and LIM/O_3 samples contain highly oxygenated and less oxygenated molecules, but LIM/O_3 SOA tends to have more fluorophores on the whole, as indicated by the higher intensity of the EEM peaks.

The APIN/OH and APIN/O_3 SOA had similar features in the EEM, but also notable differences. Common to both systems are the strong peak at E_x/E_m = 350−500/450−575 nm and a weaker peak at E_x/E_m = 250/450−500 nm, which correlate to highly oxygenated species.[39] However, APIN/O_3 SOA has two additional regions where it fluoresces: a moderate peak at E_x/E_m = 350−375/350−400 nm and a weak peak at E_x/E_m = < 300/350−400 nm. These two peaks indicate the formation of less oxygenated fluorophores from acid catalysis.[39] The APIN/OH and APIN/O_3 SOA have largely similar compounds, but in the APIN/OH system, the RO_2 + HO_2 pathway is more important, resulting in more products with hydroperoxide functionalities.[40] This could give us insights into what types of compounds have the ability to form fluorophores upon acid catalysis.

Figure 3 shows the EEM spectra for anthropogenic SOA from toluene aged under varying acidic conditions. Similar to the behavior of biogenic SOA, fluorescence is weak unless the SOA is aged in highly acidic conditions. For TOL/OH and XYL/OH samples aged in 10 M H_2SO_4 (pH −1.1), there are two regions of fluorescence: a moderate peak at E_x/E_m = 325−375/375−425 nm and a weaker peak at E_x/E_m = 300−500/425−550 nm. Compared to the biogenic photooxidation SOA, the fluorescence intensity of anthropogenic photooxidation SOA is significantly lower (by nearly an order of magnitude), with regions with the highest intensity having a difference of ∼15 QSU. The presence of these two regions implies that the fluorophores include both less and highly oxygenated

https://doi.org/10.1021/acs.jpca.4c04287
J. Phys. Chem. A 2024, 128, 7657−7668

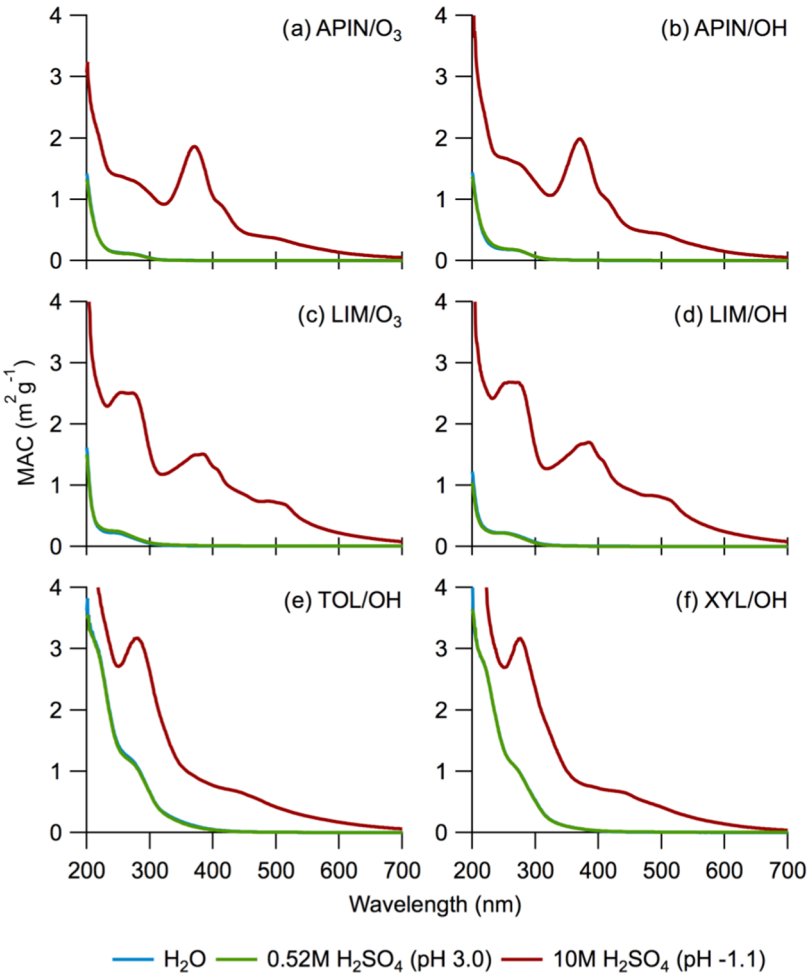

Figure 4. Mass absorption coefficient (MAC) spectra of biogenic and anthropogenic SOA aged in H_2O, 0.52 H_2SO_4 (pH 3.0), and 10 M H_2SO_4 (pH −1.1) for 2 days.

compounds, with less oxygenated fluorophores being more prevalent.[39] Based on this comparison, anthropogenic SOA do produce fluorophores upon acidic aging but less effectively compared to biogenic SOA.

Further evidence that acidity is a major driver of SOA aging is shown in Figure 4, which compares the MAC spectra of biogenic and anthropogenic SOA aged in 10 M H_2SO_4 (pH −1.1) for 2 days. For each of the samples, the MAC values of SOA aged in H_2O and 0.52 H_2SO_4 (pH 3.0) are essentially identical. However, SOA aged in 10 M H_2SO_4 (pH −1.1) shows a different spectrum, with prominent absorbance between 200 and 400 nm, and extending far in the visible range, indicating the formation of highly conjugated compounds. The overlap with the visible part of the solar spectrum is especially important: the acid-aged SOA will have a much stronger direct forcing on climate compared with the unaged one.

Fluorescence and Acid−Base Equilibria. A series of additional experiments was conducted to test the sensitivity of MAC and fluorescence spectra to acid−base equilibria. A sample of SOA aged in acid for 2 days was diluted with H_2O, and the absorption spectra were collected for each sample to monitor a shift in peak absorbance (Figure 5). The APIN systems (Figure 5a,c) exhibited a dramatic peak shift in the strong near-UV band from 370 to 310 nm. The LIM systems (Figure 5b,d) had a similar dramatic change in the shape of the MAC spectra. Specifically, the peaks at 264 and 378 nm disappeared, and a new peak grew at 239 nm upon dilution. SOA generated from anthropogenic precursors (Figure 5e,f) has a considerably smaller shift in the spectrum of the order of 6 nm. Nevertheless, it is clear that the MAC spectra are strongly pH-dependent at low pH values. We note that these shifts arise only from dilution by a factor of 4, which changes the effective pH by less than 0.5 units. This is sufficient to deprotonate the chromophore, causing a change in the absorption spectrum.

Studies have shown that atmospheric compounds have absorption spectra that are pH-dependent. For example, the spectra of nitrophenols shift to longer wavelengths at basic pH due to the formation of phenolates.[41−43] Absorption spectra of imidazole-2-carboxaldehyde and pyruvic acid solutions can be altered depending on the pH, which is prompted by complex acid−base equilibria in these systems.[20,44] Additionally, the pH dependence of the aerosol absorption has also been detected in field samples collected in the southeastern United States and Beijing.[45,46] The results presented here confirm that the absorption spectra of acid-aged SOA become very sensitive to pH in acidic particles.

The diluted samples were also analyzed by using fluorescence spectrophotometry to see if there were corresponding shifts in the EEM peaks. The resulting EEM graphs for biogenic O_3 SOA, biogenic OH SOA, and anthropogenic

https://doi.org/10.1021/acs.jpca.4c04287
J. Phys. Chem. A 2024, 128, 7657−7668

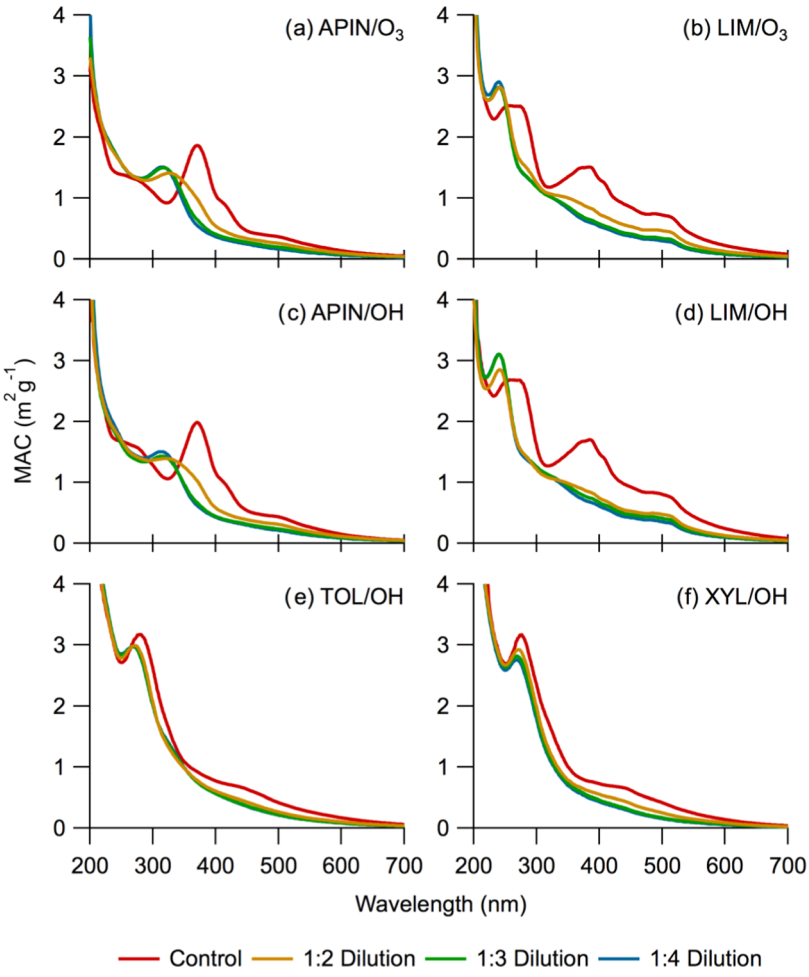

Figure 5. MAC spectra of biogenic and anthropogenic SOA aged in 10 M (pH −1.1) H_2SO_4 and then diluted with H_2O at various dilution factors.

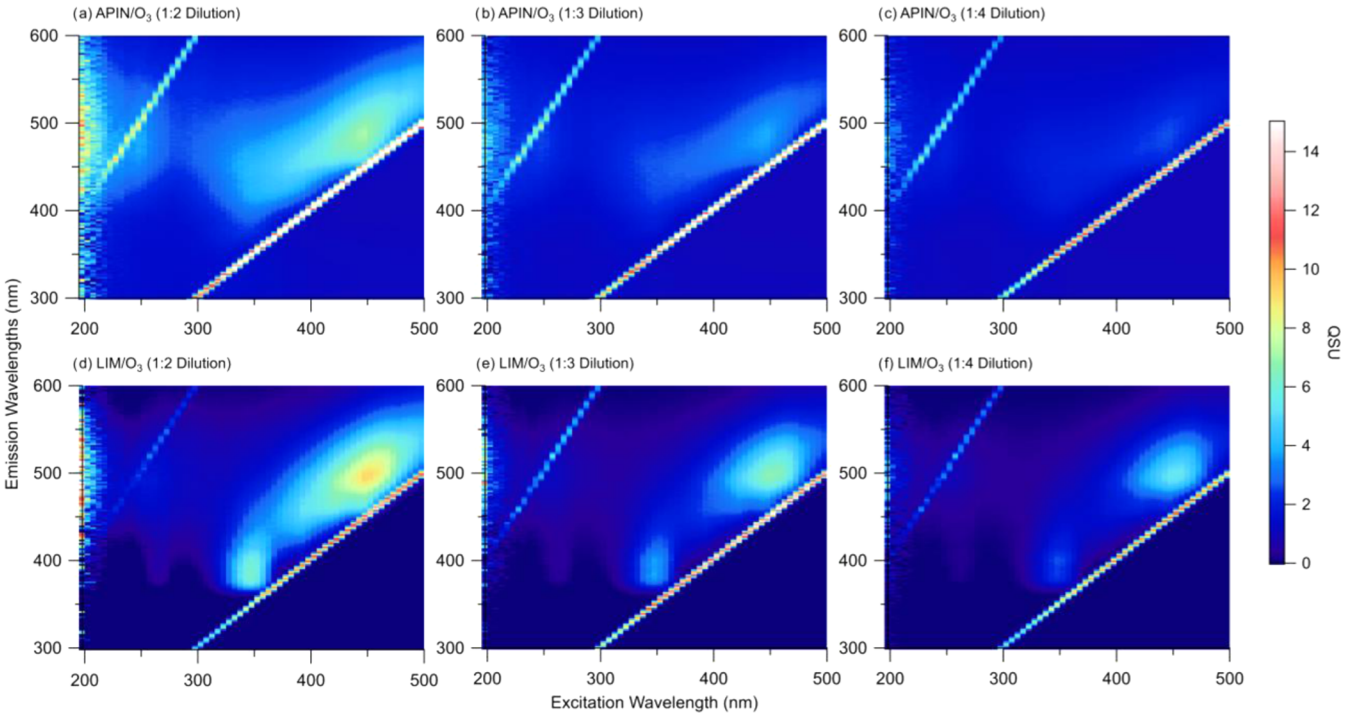

Figure 6. EEM plots for APIN/O_3 and LIM/O_3 aged in 10 M H_2SO_4 (pH −1.1) for 2 days diluted with H_2O at 1:2 (a, d), 1:3 (b, e), and 1:4 (c, f) dilution factors.

https://doi.org/10.1021/acs.jpca.4c04287
J. Phys. Chem. A 2024, 128, 7657−7668

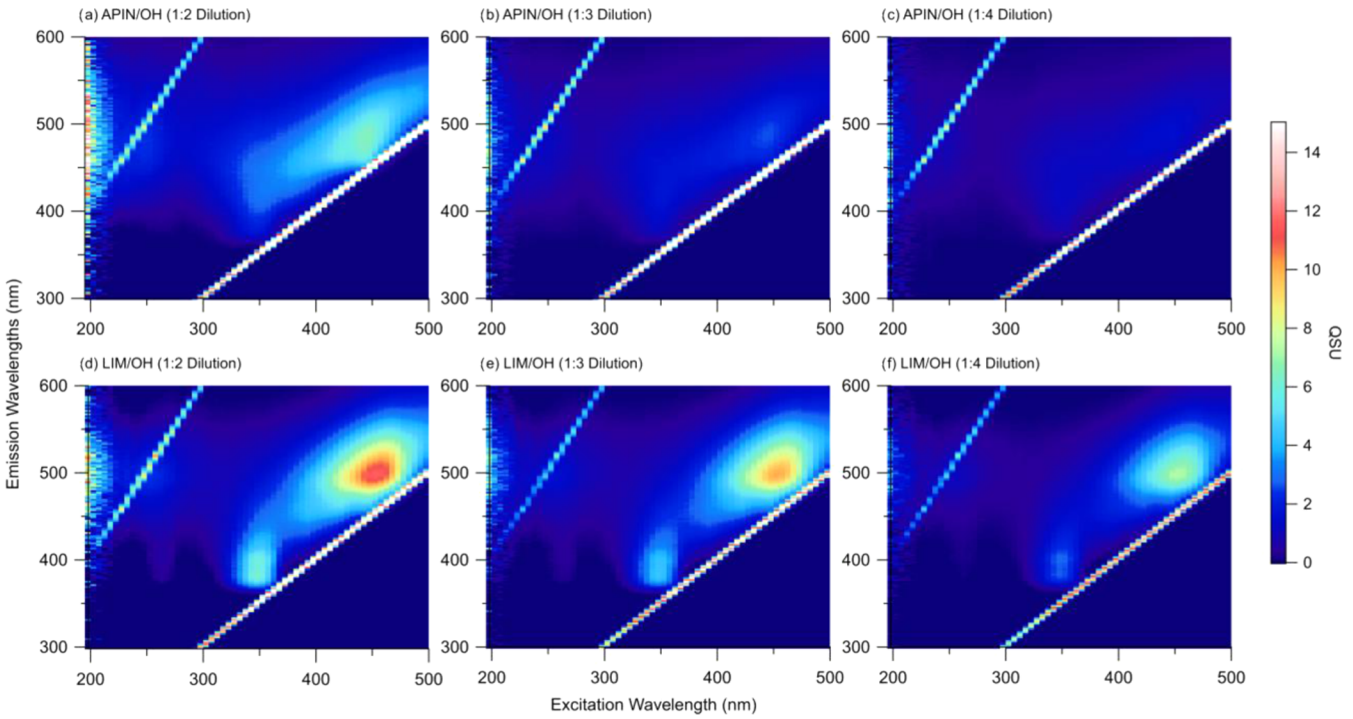

Figure 7. EEM plots for APIN/OH and LIM/OH aged in 10 M H_2SO_4 (pH − 1.1) for 2 days diluted with H_2O at 1:2 (a, d), 1:3 (b, e), and 1:4 (c, f) dilution factors.

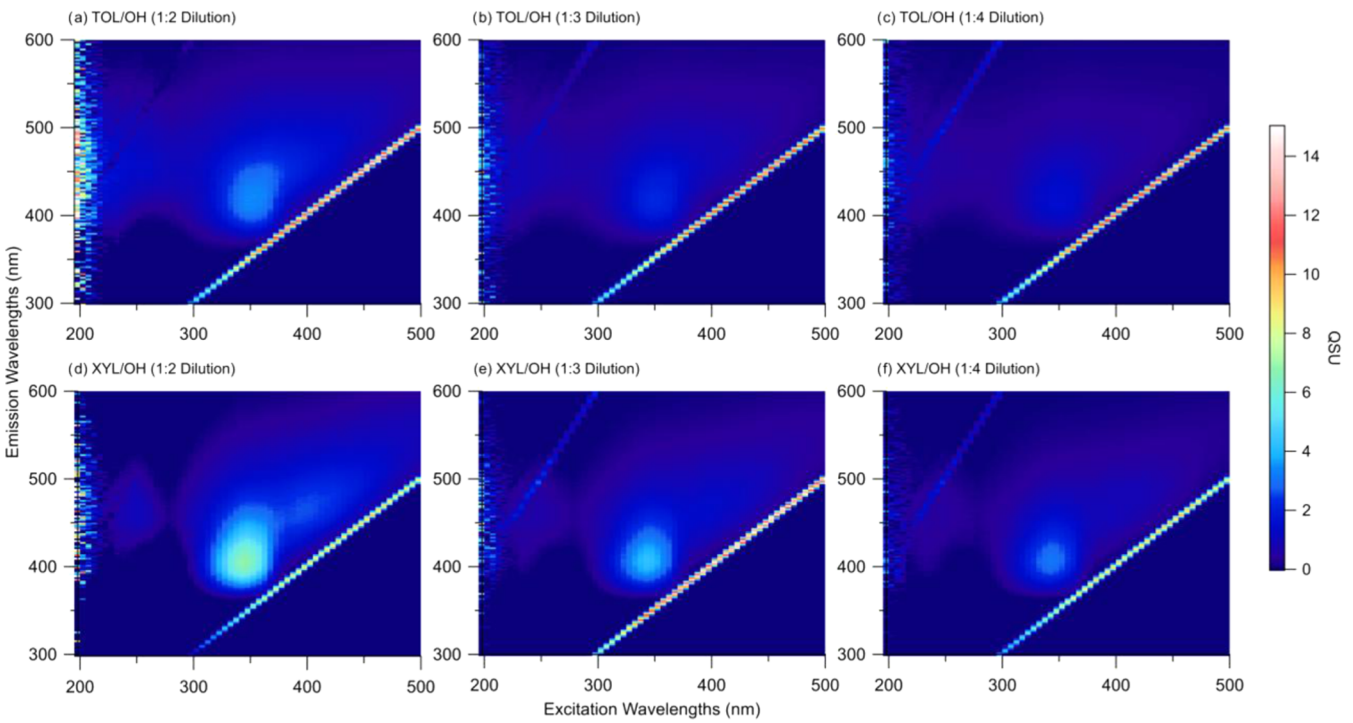

Figure 8. EEM plots for TOL/OH and XYL/OH aged in 10 M H_2SO_4 (pH −1.1) for 2 days diluted with H_2O at 1:2 (a, d), 1:3 (b, e), and 1:4 (c, f) dilution factors.

OH SOA are shown in Figures 6−8. Note that the scales differ from those in Figures 1−3 to account for the decreased intensity of fluorescence due to dilution.

The peaks in the diluted sample appeared at the same excitation and emission wavelength as in the undiluted sample (Figures 1c,f, 2c,f, and 3c,f), however, with reduced intensity due to sample dilution. No strong evidence of spectral shifts was observed, indicating that the fluorescence was not strongly affected by the acid−base equilibria after the SOA samples underwent highly acidic aging followed by dilution. To verify whether the reduced intensity in the EEM scaled with the sample dilution, the maximum fluorescence intensity of each sample was plotted against the mass concentration (Figure 9). In all cases, the maximum fluorescence intensity decreases in

https://doi.org/10.1021/acs.jpca.4c04287
J. Phys. Chem. A 2024, 128, 7657−7668

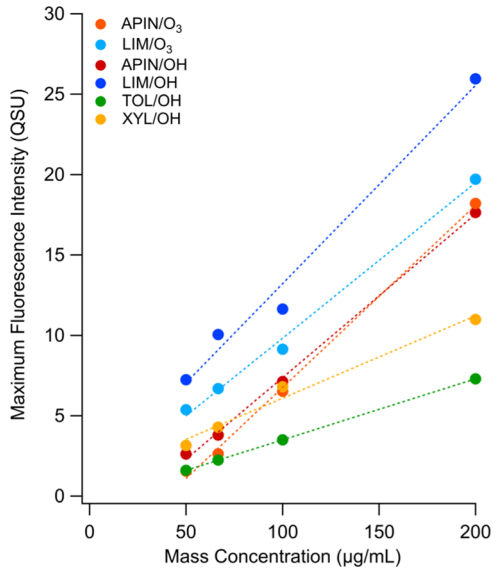

Figure 9. Maximum fluorescence intensity as a function of mass concentration for each SOA sample aged in 10 M H_2SO_4 (pH −1.1) for 2 days and then diluted with H_2O at various dilution factors.

proportion to the SOA mass concentration in the solution. This suggests that the reduced intensity is due to sample dilution rather than acid−base equilibria affecting their fluorescence. Overall, the lack of spectral shifts in the EEM data, as compared to the strong changes in the MAC spectra, suggests that the fluorophores and chromophores in these SOA systems are distinct sets of compounds that respond differently to acid−base equilibria.

Interferences with Bioaerosols. The use of fluorescence spectroscopy to carry out quantitative and qualitative analysis of PBAPs is common.[47] However, now that this study has identified the formation of fluorophores from aging SOA in highly acidic conditions, it is important to understand how these fluorophores interfere with the analysis of PBAPs. Based on the previous literature,[7] the two main classes of biological components that have similar spectral characteristics to the fluorophores formed in this study are (1) coenzymes and vitamins and (2) structural biopolymers and cell wall compounds.

Cofactors, coenzymes, and vitamins exhibit fluorescence due to heterocyclic aromatic rings within their molecular structures, such as those in pyridines, pteridines, pyridoxines, and flavins.[48,49] For example, riboflavin is a ubiquitous coenzymatic redox carrier in most organisms and is a photoreceptor in plants and fungi. Riboflavin fluoresces at E_x/E_m = 280−500/520−560 nm,[48,50−53] which overlaps with the strong fluorescence peak in the biogenic SOA at E_x/E_m = 350−500/450−575 nm. Other cofactors, coenzymes, and vitamins that interfere with the SOA fluorophores include NADPH, pyridoxine, pyridoxamine, neopterin, and ergosterol, which are found in bioaerosols derived or containing fungi, plants, microorganisms, and bacteria.[50−52,54−57]

Fluorophores can also be found in structural biopolymers and cell wall compounds, which are critical to many organisms and prevalent in the atmosphere. For instance, cellulose and chitin, which are present in plants, fungi, and algae, can fluoresce at E_x/E_m = 250−350/350−500 nm[58−60] and E_x/E_m = 335/413 nm,[61−63] respectively. However, the interference of the peak in LIM/OH, LIM/O_3, TOL/OH, and XYL/OH SOA after acidic aging at E_x/E_m = 325−375/375−425 nm can cause complications in the analysis of these spectral regions and potentially lead to an overestimation of the biological components. Therefore, it is essential for researchers to carefully consider the presence of nonbiological fluorophores in their analyses of biological components using fluorescence spectroscopy and to account for likely interference from aged SOA particles, especially if they were exposed to acidic conditions.

CONCLUSIONS

The acidity of atmospheric particles can have a large effect on the chemical processing of organic compounds in these particles and thereby their optical properties. The impacts of highly acidic conditions on the optical properties of particulate organics were explored by generating SOA from four different VOCs and aging the resulting SOA in bulk sulfuric acid solutions with atmospherically relevant acidities. We found that highly acidic conditions (corresponding to pH ∼ −1) resulted in the formation of chromophores and fluorophores after 2 days of aging, a time comparable to the residence time for aerosol particles in the atmosphere. The chromophores and fluorophores responded differently to dilution, suggesting that they represent different types of species. The mechanisms of formation of chromophores and fluorophores are unknown at this point but likely include intra- or intermolecular condensation reactions involving SOA compounds that lead to a loss of water and increase in the extent of conjugation in the condensed products.

The ability to detect and analyze fluorophores in PBAPs using fluorescence spectroscopy has proven useful for understanding the sources and types of PBAPs in the atmosphere.[9,10] However, this study has shown that acidity is a major driver of the formation of fluorophores in particles of nonbiological origin, which presents challenges for quantitative and qualitative analysis of PBAPs due to interferences from SOA.[7,11−15]

These findings may be especially important in the context of aerosol processing in the upper troposphere and lower stratosphere (UTLS). Organic compounds in UTLS particles are formed by the condensation of gas-phase precursors brought up by deep convection onto pre-existing particles.[64−66] The aerosols in this region are primarily composed of sulfuric acid (40−80 wt %), but they are also known to contain significant amounts of organic compounds.[26,27,30] These results suggest that the organic material in these particles should become fluorescent, making it hard to distinguish these particles from PBAPs by fluorescence methods. The findings from this work provide a first glimpse of how chemical reactions between sulfuric acid and organic compounds can proceed over the long lifetime of the UTLS aerosols. Further studies should include identifying the structures for chromophores and fluorophores and performing these experiments at lower temperatures representative of UTLS.

AUTHOR INFORMATION

Corresponding Author

Sergey A. Nizkorodov − *Department of Chemistry, University of California, Irvine, Irvine, California 92697-2025, United States;* orcid.org/0000-0003-0891-0052; Email: nizkorod@uci.edu

https://doi.org/10.1021/acs.jpca.4c04287
J. Phys. Chem. A 2024, 128, 7657−7668

Authors

Cynthia Wong − *Department of Chemistry, University of California, Irvine, Irvine, California 92697-2025, United States;* orcid.org/0000-0002-1597-6861

Jett Vuong − *Department of Chemistry, University of California, Irvine, Irvine, California 92697-2025, United States;* orcid.org/0009-0002-1303-2485

Complete contact information is available at: https://pubs.acs.org/10.1021/acs.jpca.4c04287

Author Contributions

The experiments and data analysis were conceived by C.W. and S.A.N. and carried out by C.W. and J.V. The manuscript was written by C.W. with contributions from all the coauthors. All authors have given approval to the final version of the manuscript.

Notes

The authors declare no competing financial interest.

■ ACKNOWLEDGMENTS

The UCI team acknowledges the financial support from NSF grant AGS-2334731. C.W. acknowledges the support from the Ridge to Reef NSF Research Traineeship, award DGE-1735040.

■ REFERENCES

(1) Jimenez, J. L.; Canagaratna, M. R.; Donahue, N. M.; Prevot, A. S. H.; Zhang, Q.; Kroll, J. H.; DeCarlo, P. F.; Allan, J. D.; Coe, H.; Ng, N. L.; et al. Evolution of Organic Aerosols in the Atmosphere. *Science* **2009**, *326* (5959), 1525−1529.

(2) Després, V. R.; Alex Huffman, J.; Burrows, S. M.; Hoose, C.; Safatov, A. S.; Buryak, G.; Fröhlich-Nowoisky, J.; Elbert, W.; Andreae, M. O.; Pöschl, U.; Jaenicke, R. Primary Biological Aerosol Particles in the Atmosphere: A Review. *Tellus B* **2022**, *64* (1), No. 15598, DOI: 10.3402/TELLUSB.V64I0.15598.

(3) Ervens, B.; Turpin, B. J.; Weber, R. J. Secondary Organic Aerosol Formation in Cloud Droplets and Aqueous Particles (AqSOA): A Review of Laboratory, Field and Model Studies. *Atmos. Chem. Phys.* **2011**, *11* (21), 11069−11102.

(4) Kanakidou, M.; Seinfeld, J. H.; Pandis, S. N.; Barnes, I.; Dentener, F. J.; Facchini, M. C.; Van Dingenen, R.; Ervens, B.; Nenes, A.; Nielsen, C. J.; et al. J. Organic Aerosol and Global Climate Modelling: A Review. *Atmos. Chem. Phys.* **2005**, 1053−1123.

(5) Pan, Y. Le. Detection and Characterization of Biological and Other Organic-Carbon Aerosol Particles in Atmosphere Using Fluorescence. *J. Quant. Spectrosc. Radiat. Transfer* **2015**, *150*, 12−35.

(6) Graber, E. R.; Rudich, Y. Atmospheric HULIS: How Humic-like Are They? A Comprehensive and Critical Review. *Atmos. Chem. Phys.* **2006**, *6* (3), 729−753.

(7) Pöhlker, C.; Huffman, J. A.; Pöschl, U. Autofluorescence of Atmospheric Bioaerosols - Fluorescent Biomolecules and Potential Interferences. *Atmos. Meas. Tech.* **2012**, *5* (1), 37−71.

(8) Laskin, A.; Laskin, J.; Nizkorodov, S. A. Chemistry of Atmospheric Brown Carbon. *Chem. Rev.* **2015**, *115* (10), 4335−4382.

(9) Chen, Q.; Mu, Z.; Song, W.; Wang, Y.; Yang, Z.; Zhang, L.; Zhang, Y. L. Size-Resolved Characterization of the Chromophores in Atmospheric Particulate Matter From a Typical Coal-Burning City in China. *J. Geophys. Res.: Atmos.* **2019**, *124* (19), 10546−10563.

(10) Barsotti, F.; Ghigo, G.; Vione, D. Computational Assessment of the Fluorescence Emission of Phenol Oligomers: A Possible Insight into the Fluorescence Properties of Humic-like Substances (HULIS). *J. Photochem. Photobiol., A* **2016**, *315*, 87−93.

(11) Bones, D. L.; Henricksen, D. K.; Mang, S. A.; Gonsior, M.; Bateman, A. P.; Nguyen, T. B.; Cooper, W. J.; Nizkorodov, S. A. Appearance of Strong Absorbers and Fluorophores in Limonene-O_3 Secondary Organic Aerosol Due to NH_4^+-Mediated Chemical Aging over Long Time Scales. *J. Geophys. Res.: Atmos.* **2010**, *115* (D5), 5203.

(12) Aiona, P. K.; Luek, J. L.; Timko, S. A.; Powers, L. C.; Gonsior, M.; Nizkorodov, S. A. Effect of Photolysis on Absorption and Fluorescence Spectra of Light-Absorbing Secondary Organic Aerosols. *ACS Earth Space Chem.* **2018**, *2* (3), 235−245.

(13) Lee, H. J. J.; Laskin, A.; Laskin, J.; Nizkorodov, S. A. Excitation-Emission Spectra and Fluorescence Quantum Yields for Fresh and Aged Biogenic Secondary Organic Aerosols. *Environ. Sci. Technol.* **2013**, *47* (11), 5763−5770.

(14) Ammor, M. S. Recent Advances in the Use of Intrinsic Fluorescence for Bacterial Identification and Characterization. *J. Fluoresc.* **2007**, *17* (5), 455−459.

(15) Negron, A.; Deleon-Rodriguez, N.; Waters, S. M.; Ziemba, L. D.; Anderson, B.; Bergin, M.; Konstantinidis, K. T.; Nenes, A. Using Flow Cytometry and Light-Induced Fluorescence to Characterize the Variability and Characteristics of Bioaerosols in Springtime in Metro Atlanta, Georgia. *Atmos Chem Phys* **2020**, *20* (3), 1817−1838.

(16) Luo, M.; Shemesh, D.; Sullivan, M. N.; Alves, M. R.; Song, M.; Gerber, R. B.; Grassian, V. H. Impact of pH and NaCl and $CaCl_2$ Salts on the Speciation and Photochemistry of Pyruvic Acid in the Aqueous Phase. *J. Phys. Chem. A* **2020**, *124* (25), 5071−5080.

(17) Karimova, N. V.; Luo, M.; Grassian, V. H.; Gerber, R. B. Absorption Spectra of Benzoic Acid in Water at Different pH and in the Presence of Salts: Insights from the Integration of Experimental Data and Theoretical Cluster Models. *Phys. Chem. Chem. Phys.* **2020**, *22* (9), 5046−5056.

(18) Pye, H. O. T.; Nenes, A.; Alexander, B.; Ault, A. P.; Barth, M. C.; Clegg, S. L.; Collett, J. L.; Fahey, K. M.; Hennigan, C. J.; Herrmann, H.; et al. The Acidity of Atmospheric Particles and Clouds. *Atmos. Chem. Phys.* **2020**, *20*, 4809−4888.

(19) Angle, K. J.; Crocker, D. R.; C Simpson, R. M.; Mayer, K. J.; Garofalo, L. A.; Moore, A. N.; Mora Garcia, S. L.; Or, V. W.; Srinivasan, S.; Farhan, M.; et al. Acidity across the Interface from the Ocean Surface to Sea Spray Aerosol. *Proc. Natl. Acad. Sci. U.S.A.* **2021**, *118* (2), No. e2018397118, DOI: 10.1073/pnas.2018397118.

(20) Tilgner, A.; Schaefer, T.; Alexander, B.; Barth, M. C.; Collett, J. L.; Fahey, K. M.; Nenes, A.; Pye, H. O. T.; Herrmann, H.; McNeill, V. F. Acidity and the Multiphase Chemistry of Atmospheric Aqueous Particles and Clouds. *Atmos. Chem. Phys.* **2021**, *21* (17), 13483−13536.

(21) Battaglia, M. A.; Douglas, S.; Hennigan, C. J. Effect of the Urban Heat Island on Aerosol pH. *Environ. Sci. Technol.* **2017**, *51* (22), 13095−13103.

(22) Guo, H.; Sullivan, A. P.; Campuzano-Jost, P.; Schroder, J. C.; Lopez-Hilfiker, F. D.; Dibb, J. E.; Jimenez, J. L.; Thornton, J. A.; Brown, S. S.; Nenes, A.; Weber, R. J. Fine Particle pH and the Partitioning of Nitric Acid during Winter in the Northeastern United States. *J. Geophys. Res.: Atmos.* **2016**, *121* (17), 10355−10376.

(23) Guo, H.; Xu, L.; Bougiatioti, A.; Cerully, K. M.; Capps, S. L.; Hite, J. R.; Carlton, A. G.; Lee, S. H.; Bergin, M. H.; Ng, N. L.; et al. Fine-Particle Water and pH in the Southeastern United States. *Atmos. Chem. Phys.* **2015**, *15* (9), 5211−5228.

(24) Cheng, C.; Wang, G.; Meng, J.; Wang, Q.; Cao, J.; Li, J.; Wang, J. Size-Resolved Airborne Particulate Oxalic and Related Secondary Organic Aerosol Species in the Urban Atmosphere of Chengdu, China. *Atmos. Res.* **2015**, *161*−*162*, 134−142.

(25) Clegg, S. L.; Brimblecombe, P.; Wexler, A. S. Thermodynamic Model of the System H^+−NH_4^+−SO_4^{2-}−NO_3^-−H_2O at Tropospheric Temperatures. *J. Phys. Chem. A* **1998**, *102* (12), 2137−2154.

(26) Tabazadeh, A.; Toon, O. B.; Clegg, S. L.; Hamill, P. A New Parameterization of H_2SO_4/H_2O Aerosol Composition: Atmospheric Implications. *Geophys. Res. Lett.* **1997**, *24* (15), 1931−1934.

(27) Froyd, K. D.; Murphy, D. M.; Sanford, T. J.; Thomson, D. S.; Wilson, J. C.; Pfister, L.; Lait, L. Aerosol Composition of the Tropical Upper Troposphere. *Atmos. Chem. Phys.* **2009**, *9* (13), 4363−4385.

(28) Murphy, D. M.; Thomson, D. S.; Mahoney, M. J. In Situ Measurements of Organics, Meteoritic Material, Mercury, and Other

Elements in Aerosols at 5 to 19 Kilometers. *Science* **1998**, *282* (5394), 1664−1669.
(29) Murphy, D. M.; Froyd, K. D.; Schwarz, J. P.; Wilson, J. C. Observations of the Chemical Composition of Stratospheric Aerosol Particles. *Q. J. R. Meteorol. Soc.* **2014**, *140* (681), 1269−1278.
(30) Murphy, D. M.; Cziczo, D. J.; Hudson, P. K.; Thomson, D. S. Carbonaceous Material in Aerosol Particles in the Lower Stratosphere and Tropopause Region. *J. Geophys. Res.: Atmos.* **2007**, *112*, No. D04203.
(31) Wong, C.; Liu, S.; Nizkorodov, S. A. Highly Acidic Conditions Drastically Alter the Chemical Composition and Absorption Coefficient of α-Pinene Secondary Organic Aerosol. *ACS Earth Space Chem.* **2022**, *6* (12), 2983−2994.
(32) Wong, C.; Vite, D.; Nizkorodov, S. A. Stability of α-Pinene and d -Limonene Ozonolysis Secondary Organic Aerosol Compounds Toward Hydrolysis and Hydration. *ACS Earth Space Chem.* **2021**, *5* (10), 2555−2564.
(33) Baboomian, V. J.; Gu, Y.; Nizkorodov, S. A. Photodegradation of Secondary Organic Aerosols by Long-Term Exposure to Solar Actinic Radiation. *ACS Earth Space Chem.* **2020**, *4* (7), 1078−1089.
(34) Veghte, D. P.; China, S.; Weis, J.; Lin, P.; Hinks, M. L.; Kovarik, L.; Nizkorodov, S. A.; Gilles, M. K.; Laskin, A. Heating-Induced Transformations of Atmospheric Particles: Environmental Transmission Electron Microscopy Study. *Anal. Chem.* **2018**, *90* (16), 9761−9768.
(35) Timko, S. A.; Maydanov, A.; Pittelli, S. L.; Conte, M. H.; Cooper, W. J.; Koch, B. P.; Schmitt-Kopplin, P.; Gonsior, M. Depth-Dependent Photodegradation of Marine Dissolved Organic Matter. *Front. Mar. Sci.* **2015**, *2*, 66.
(36) Zepp, R. G.; Sheldon, W. M.; Moran, M. A. Dissolved Organic Fluorophores in Southeastern US Coastal Waters: Correction Method for Eliminating Rayleigh and Raman Scattering Peaks in Excitation−Emission Matrices. *Mar. Chem.* **2004**, *89* (1−4), 15−36.
(37) Duarte, R. M. B. O.; Pio, C. A.; Duarte, A. C. Synchronous Scan and Excitation-Emission Matrix Fluorescence Spectroscopy of Water-Soluble Organic Compounds in Atmospheric Aerosols. *J. Atmos. Chem.* **2004**, *48* (2), 157−171.
(38) Laskin, J.; Laskin, A.; Nizkorodov, S. A.; Roach, P.; Eckert, P.; Gilles, M. K.; Wang, B.; Lee, H. J.; Hu, Q. Molecular Selectivity of Brown Carbon Chromophores. *Environ. Sci. Technol.* **2014**, *48* (20), 12047−12055.
(39) Chen, Q.; Miyazaki, Y.; Kawamura, K.; Matsumoto, K.; Coburn, S.; Volkamer, R.; Iwamoto, Y.; Kagami, S.; Deng, Y.; Ogawa, S.; et al. Characterization of Chromophoric Water-Soluble Organic Matter in Urban, Forest, and Marine Aerosols by HR-ToF-AMS Analysis and Excitation-Emission Matrix Spectroscopy. *Environ. Sci. Technol.* **2016**, *50* (19), 10351−10360.
(40) Zhang, X.; McVay, R. C.; Huang, D. D.; Dalleska, N. F.; Aumont, B.; Flagan, R. C.; Seinfeld, J. H. Formation and Evolution of Molecular Products in α-Pinene Secondary Organic Aerosol. *Proc. Natl. Acad. Sci. U.S.A.* **2015**, *112* (46), 14168−14173.
(41) Vione, D.; Maurino, V.; Minero, C.; Duncianu, M.; Olariu, R. I.; Arsene, C.; Sarakha, M.; Mailhot, G. Assessing the Transformation Kinetics of 2- and 4-Nitrophenol in the Atmospheric Aqueous Phase. Implications for the Distribution of Both Nitroisomers in the Atmosphere. *Atmos. Environ.* **2009**, *43* (14), 2321−2327.
(42) Barsotti, F.; Bartels-Rausch, T.; De Laurentiis, E.; Ammann, M.; Brigante, M.; Mailhot, G.; Maurino, V.; Minero, C.; Vione, D. Photochemical Formation of Nitrite and Nitrous Acid (HONO) upon Irradiation of Nitrophenols in Aqueous Solution and in Viscous Secondary Organic Aerosol Proxy. *Environ. Sci. Technol.* **2017**, *51* (13), 7486−7495.
(43) Lee, H. J. J.; Aiona, P. K.; Laskin, A.; Laskin, J.; Nizkorodov, S. A. Effect of Solar Radiation on the Optical Properties and Molecular Composition of Laboratory Proxies of Atmospheric Brown Carbon. *Environ. Sci. Technol.* **2014**, *48* (17), 10217−10226.
(44) Ackendorf, J. M.; Ippolito, M. G.; Galloway, M. M. pH Dependence of the Imidazole-2-Carboxaldehyde Hydration Equilibrium: Implications for Atmospheric Light Absorbance. *Environ. Sci. Technol. Lett.* **2017**, *4* (12), 551−555.
(45) Phillips, S. M.; Bellcross, A. D.; Smith, G. D. Light Absorption by Brown Carbon in the Southeastern United States Is pH-Dependent. *Environ. Sci. Technol.* **2017**, *51* (12), 6782−6790.
(46) Qin, J.; Zhang, L.; Qin, Y.; Shi, S.; Li, J.; Gao, Y.; Tan, J.; Wang, X. pH-Dependent Chemical Transformations of Humic-Like Substances and Further Cognitions Revealed by Optical Methods. *Environ. Sci. Technol.* **2022**, *56* (12), 7578−7587.
(47) Huffman, J. A.; Perring, A. E.; Savage, N. J.; Clot, B.; Crouzy, B.; Tummon, F.; Shoshanim, O.; Damit, B.; Schneider, J.; Sivaprakasam, V.; Zawadowicz, M. A.; Crawford, I.; Gallagher, M.; Topping, D.; Doughty, D. C.; Hill, S. C.; Pan, Y. Real-Time Sensing of Bioaerosols: Review and Current Perspectives. *Aerosol Sci. Technol.* **2020**, *54* (5), 465−495.
(48) Wlodarski, M.; Kaliszewski, M.; Kwasny, M.; Kopczynski, K.; Zawadzki, Z.; Wlodarski, A. M.; Mierczyk, Z.; Mlynczak, J.; Trafny, E.; Szpakowska, M. In *Fluorescence Excitation-Emission Matrices of Selected Biological Materials*, Optically Based Biological and Chemical Detection for Defence III, SPIE, 2006; pp 11−22.
(49) Dalterio, R. A.; Nelson, W. H.; Britt, D.; Sperry, J. F.; Tanguay, J. F.; Suib, S. L. The Steady-State and Decay Characteristics of Primary Fluorescence from Live Bacteria. *Appl. Spectrosc.* **1987**, *41* (2), 234−241.
(50) Kopczynski, K.; Kwasny, M.; Mierczyk, Z.; Zawadzki, K.; Kopczynski, Z.; Zawadzki, Z. Laser Induced Fluorescence System for Detection of Biological Agents: European Project FABIOLA. In *Optical Security Systems*; SPIE, 2005; Vol. *5954*, pp 30−41.
(51) Ramanujam, N. Fluorescence Spectroscopy of Neoplastic and Non-Neoplastic Tissues. *Neoplasia* **2000**, *2* (1−2), 89.
(52) Billinton, N.; Knight, A. W. Seeing the Wood through the Trees: A Review of Techniques for Distinguishing Green Fluorescent Protein from Endogenous Autofluorescence. *Anal. Biochem.* **2001**, *291* (2), 175−197.
(53) Benson, R. C.; Meyer, R. A.; Zaruba, M. E.; McKhann, G. M. Cellular Autofluorescence–Is It Due to Flavins? *J. Histochem. Cytochem.* **1979**, *27* (1), 44−48.
(54) Richards-Kortum, R.; Sevick-Muraca, E. Quantitative Optical Spectroscopy for Tissue Diagnosis. *Annu. Rev. Phys. Chem.* **1996**, *47*, 555−606.
(55) Avi-Dor, Y.; Olson, J. M.; Doherty, M. D.; Kaplan, N. O. Fluorescence of Pyridine Nucleotides in Mitochondria. *J. Biol. Chem.* **1962**, *237* (7), 2377−2383.
(56) Bueno, C.; Encinas, M. V. Photophysical and Photochemical Studies of Pyridoxamine. *Helv. Chim. Acta* **2003**, *86* (10), 3363−3375.
(57) Ramanujam, N. Fluorescence Spectroscopy In Vivo. In *Encyclopedia of Analytical Chemistry*; Wiley, 2006.
(58) Olmstead, J. A.; Gray, D. G. Fluorescence Emission from Mechanical Pulp Sheets. *J. Photochem. Photobiol., A* **1993**, *73* (1), 59−65.
(59) Castellan, A.; Ruggiero, R.; Frollini, E.; Ramos, L. A.; Chirat, C. Studies on Fluorescence of Cellulosics. *Holzforschung* **2007**, *61* (5), 504−508.
(60) Olmstead, J. A.; Gray, D. G. Fluorescence Spectroscopy of Cellulose, Lignin and Mechanical Pulps: A Review. *J. Pulp Pap. Sci.* **1997**, *23* (12), J571−J581.
(61) Dreyer, B.; Morte, A.; Pérez-Gilabert, M.; Honrubia, M. Autofluorescence Detection of Arbuscular Mycorrhizal Fungal Structures in Palm Roots: An Underestimated Experimental Method. *Mycol. Res.* **2006**, *110* (8), 887−897.
(62) Bonfante-Fasolo, P.; Faccio, A.; Perotto, S.; Schubert, A. Correlation between Chitin Distribution and Cell Wall Morphology in the Mycorrhizal Fungus Glomus Versiforme. *Mycol. Res.* **1990**, *94* (2), 157−165.
(63) Vierheiling, H.; Böckenhoff, A.; Knoblauch, M.; Juge, C.; Van Bel, A. J. E.; Grundler, F.; Piché, Y.; Wyss, U. In Vivo Observations of the Arbuscular Mycorrhizal Fungus Glomus Mosseae in Roots by Confocal Laser Scanning Microscopy. *Mycol. Res.* **1999**, *103* (3), 311−314.

https://doi.org/10.1021/acs.jpca.4c04287
J. Phys. Chem. A 2024, 128, 7657−7668

(64) Andreae, M. O.; Afchine, A.; Albrecht, R.; Amorim Holanda, B.; Artaxo, P.; Barbosa, H. M. J.; Borrmann, S.; Cecchini, M. A.; Costa, A.; Dollner, M.; et al. Aerosol Characteristics and Particle Production in the Upper Troposphere over the Amazon Basin. *Atmos. Chem. Phys.* **2018**, *18* (2), 921−961.
(65) Twohy, C. H.; Clement, C. F.; Gandrud, B. W.; Weinheimer, A. J.; Campos, T. L.; Baumgardner, D.; Brune, W. H.; Faloona, I.; Sachse, G. W.; Vay, S. A.; Tan, D. Deep Convection as a Source of New Particles in the Midlatitude Upper Troposphere. *J. Geophys. Res.: Atmos.* **2002**, *107* (D21), No. AAC6-1.
(66) Weigel, R.; Borrmann, S.; Kazil, J.; Minikin, A.; Stohl, A.; Wilson, J. C.; Reeves, J. M.; Kunkel, D.; De Reus, M.; Frey, W.; et al. In Situ Observations of New Particle Formation in the Tropical Upper Troposphere: The Role of Clouds and the Nucleation Mechanism. *Atmos. Chem. Phys.* **2011**, *11* (18), 9983−10010.

https://doi.org/10.1021/acs.jpca.4c04287
J. Phys. Chem. A 2024, 128, 7657−7668